OXFORD

Human Molecular Genetics, 2016, Vol. 0, No. 0 1–9

doi: 10.1093/hmg/ddw372
Advance Access Publication Date: 26 November 2016
Original Article

ORIGINAL ARTICLE

Transgenic *TBK1* mice have features of normal tension glaucoma

John H. Fingert[1,2,*], Kathy Miller[1,2], Adam Hedberg-Buenz[1,2,3], Ben R. Roos[1,2], Carly J. Lewis[1,2,3], Robert F. Mullins[1,2] and Michael G. Anderson[1,2,3,4]

[1]Department of Ophthalmology and Visual Sciences, Carver College of Medicine, University of Iowa, Iowa City, IA, USA, [2]Stephen A. Wynn Institute for Vision Research, University of Iowa, Iowa City, IA, USA, [3]Department of Molecular Physiology and Biophysics, Carver College of Medicine, University of Iowa, Iowa City, IA, USA and [4]VA Center for the Prevention and Treatment of Visual Loss, Iowa City VA Health Care System, Iowa City, IA, USA

*To whom correspondence should be addressed at: John H. Fingert, University of Iowa, 3111B MERF, 375 Newton Road, Iowa City, IA 52242, USA. Tel: 319-335-7508; Fax: 877-434-9041; Email: john-fingert@uiowa.edu

Abstract

Duplication of the *TBK1* gene is associated with 1–2% of normal tension glaucoma, a common cause of vision loss and blindness that occurs without grossly abnormal intraocular pressure. We generated a transgenic mouse that has one copy of the human *TBK1* gene (native promoter and gene structure) incorporated into the mouse genome (Tg-*TBK1*). Expression of the *TBK1* transgene in the retinae of these mice was demonstrated by real-time PCR. Using immunohistochemistry TBK1 protein was predominantly localized to the ganglion cell layer of the retina, the cell type most affected by glaucoma. More intense TBK1 labelling was detected in the retinal ganglion cells (RGCs) of Tg-*TBK1* mice than in wild-type littermates. Tg-*TBK1* mice exhibit the cardinal sign of glaucoma, a progressive loss of RGCs. Hemizygous Tg-*TBK1* mice (with one *TBK1* transgene per genome) had a 13% loss of RGCs by 18 months of age ($P = 1.5 \times 10^{-8}$). Homozygous Tg-*TBK1* mice had 7.6% fewer RGCs than hemizygous Tg-*TBK1* mice and 20% fewer RGCs than wild-type mice ($P = 1.9 \times 10^{-5}$) at 6 months of age. No difference in intraocular pressures was detected between Tg-*TBK1* mice and wild-type littermates as they aged ($P > 0.05$). Tg-*TBK1* mice with extra doses of the *TBK1* gene recapitulate the phenotype of normal tension glaucoma in human patients with a *TBK1* gene duplication. Together, these studies confirm the pathogenicity of the *TBK1* gene duplication in human glaucoma and suggest that excess production of TBK1 kinase may have a role in the pathology of glaucoma.

Introduction

Primary open angle glaucoma (POAG) is the most common form of glaucoma worldwide and is a common cause of blindness and visual disability (1). The chief features of POAG are a characteristic pattern of optic nerve damage (cupping of the optic disc) and a corresponding, characteristic pattern of visual field loss. Elevated intraocular pressure (IOP) is a risk factor for glaucoma, however, the disease can occur at any IOP. When POAG occurs in the absence of elevated IOP it is frequently termed normal tension glaucoma (NTG). The overall prevalence of POAG ranges from 0.5 to 8.8% depending on age, ethnicity and diagnostic criteria employed and 30–92% of these POAG patients may be classified as NTG (2). NTG accounts for a significant proportion of glaucoma worldwide that is higher in Asian populations (76%) than in white populations (34%) (3).

Genetic variation is important in the pathogenesis of glaucoma. Some cases of POAG have a complex genetic basis and are caused by the combined actions of many genetic risk factors and environmental factors (4). Genome-wide association studies have identified many of these genetic risk factors for POAG including the following genes and loci: *CAV1/CAV2* (5),

Received: September 13, 2016. **Revised:** October 23, 2016. **Accepted:** October 25, 2016

CDKN2B-AS1 (6), *TMCO1* (6), *ATOH7* (7), *SIX1/SIX6* (7), *SALL1* (7), *CDC7/TGFBR3* (7), chromosome 8q22 (8), *CHEK2* (9), *ABCA1* (10), *ARHGEF12* (10), *GMDS* (10), *PMM2* (11), *FNDC3B* (12), *TXNRD2* (13), *ATXN2* (13) and *FOXC1* (13). A different, but overlapping set of risk factors for NTG has also been discovered: *ELOVL5* (14), *SRBD1* (14), *TLR4* (15) and *CDKN2B-AS1* (16,17). Many of these genes have roles in biological processes that may contribute to the pathogenesis of glaucoma including ocular development (*SIX1/SIX6* and *FOXC1*), TGF-β signalling (*CDKN2B-AS1* and *TGFBR3*) and regulation of autophagy (*ATXN2*) (18).

Other cases of POAG are caused primarily by a single mutation in one of several known glaucoma genes. Missense and nonsense mutations in the myocilin (*MYOC*) gene have been associated with autosomal dominant inheritance of glaucoma with high IOP in both juvenile- and adult-onset forms of POAG (19–21). In contrast, mutations in the optineurin (*OPTN*) gene (22–26) and in the TANK-binding kinase 1 (*TBK1*) gene (27–31) have been associated with NTG, glaucoma that occurs with low or average IOP. One specific mutation in *OPTN*, E50K, has been associated with 1–2% of NTG cases in many patient populations (23,24,32). Similarly, *TBK1* gene duplications and triplications have been associated with ∼1% of NTG cases including African American (27), Caucasian (27,29–31) and Asian patients (28). One example of a *TBK1* gene deletion has been reported in a glaucoma patient (31). The specific mechanism by which mutations in *OPTN* and *TBK1* cause NTG is unknown. However, both genes encode proteins that participate in the same biological pathways, NF-κB signalling and autophagy.

Autophagy is a cellular process that delivers cytosolic proteins, organelles and even intracellular pathogens to lysosomes for degradation and clearance. Autophagy can protect cells by providing energy in times of nutrient deprivation or as a means to degrade dysfunctional organelles (e.g. damaged mitochondria) or intracellular pathogens (33). Excessive autophagy can also lead to a form of programmed cell death. Alterations in autophagy have also been described in several experimental animal models of glaucoma (34–36). More recently, retinal ganglion cell-like neurons were produced from patient skin biopsies and induced pluripotent stem cells (iPSCs). Retinal ganglion cell-like neurons from patients with NTG were shown to have activated autophagy associated with a *TBK1* gene duplication (37). These data suggest that some fraction of NTG cases may be caused in part by dysregulation of autophagy. Autophagy has also been implicated in other neurodegenerative diseases such as Alzheimer's Disease, Parkinson's Disease and amyotrophic lateral sclerosis (ALS) (38). Interestingly, different sets of mutations in the same autophagy genes that cause or contribute to NTG (*TBK1, OPTN* and *ATXN2*) have been implicated in the pathogenesis of ALS (39–42) suggesting possible links between glaucoma and other degenerative neurological conditions.

Copy number variation (CNV) mutations of the *TBK1* gene have been detected in several different populations of NTG patients from around the world and have not been identified in control subjects or public databases (27–31). Moreover, *TBK1* is most highly expressed at the site of ocular pathology in NTG, the ganglion cell layer and nerve fibre layer of the retina (27). Furthermore, *TBK1* gene duplications are known to result in increased expression of the *TBK1* gene (27). These data have suggested that *TBK1* CNVs cause increased gene expression and by dysregulating autophagy may ultimately lead to retinal ganglion cell death and glaucoma (37). In this report, we further explore the role of *TBK1* gene duplications in the pathophysiology of NTG by engineering and characterizing a transgenic mouse with the same genetic defect carried by humans with *TBK1*-associated glaucoma. We generated a transgenic strain of mice that has one wild-type copy of the human *TBK1* gene and its native promoter incorporated into its genome (Tg-*TBK1*). The Tg-*TBK1* mice have a total of three of these kinase genes in their genome (one human *TBK1* transgene and two native *Tbk1* genes). Here we investigate the Tg-*TBK1* mice for a recapitulation of the glaucoma phenotype observed in human NTG patients, which would provide the strongest evidence that *TBK1* gene duplications do in fact cause NTG.

Results

Generation of transgenic (Tg-*TBK1*) mice

We previously discovered that copy number variations of the *TBK1* gene (i.e. duplications or triplications) are associated with NTG (27). Our subsequent studies showed that *TBK1* mutations are responsible for approximately 1% of cases of NTG (28–31). The pathogenicity of *TBK1* copy number variations is supported by their presence in patients with NTG, their absence in control subjects, and their absence in public databases (27–31). However, in order to provide stronger evidence that *TBK1* gene duplications cause NTG, we generated a transgenic mouse with an extra copy of the *TBK1* gene in an attempt to recapitulate human NTG in the mouse. A bacterial artificial chromosome (BAC) containing the entire human *TBK1* gene (promoter, exons and introns) was obtained from BACPAC (RP11-60O8, Oakland, CA) and used as a vector to produce transgenic mice. Mice carrying the transgene were identified and genotyped with a quantitative real-time PCR assay for the *TBK1* gene (Fig. 1). One founder was identified that carried a single copy of the human *TBK1* gene and was reiteratively backcrossed against C57BL/6J to produce the line B6.Tg(*TBK1*), which has one copy of the human *TBK1* transgene in addition to the two copies of the mouse orthologue *Tbk1* in its genome. These mice are hereafter referred to as 'Tg-*TBK1* mice'.

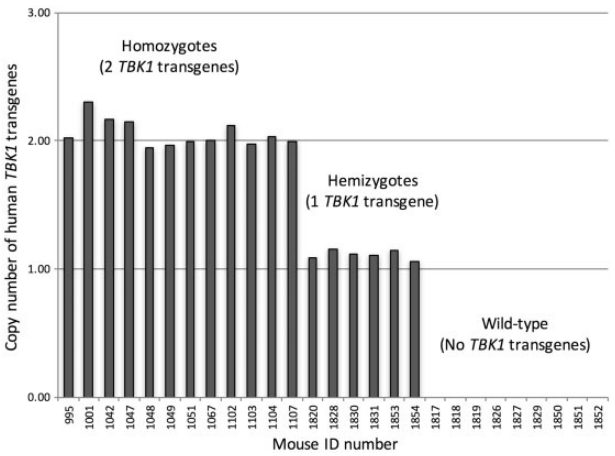

Figure 1. Tg-*TBK1* mice carry the human *TBK1* transgene. Mice were genotyped using a quantitative real-time PCR assay to identify animals that carried the human *TBK1* transgene. Approximately half the mice carried one copy of the transgene in their genome, while the half had no copies of the transgene. Genotyping offspring from an intercross of Tg-*TBK1* mice with quantitative PCR identified mice that have two copies of the *TBK1* transgene (homozygotes); mice that have one copy of the *TBK1* transgene (hemizygotes); and wild-type mice with no copies of the transgene (above).

Ocular production of *TBK1*

Quantitative real-time PCR with probes specific for the mouse *Tbk1* mRNA was used to assess expression of the native mouse *Tbk1* gene in retinae from three Tg-*TBK1* mice and from three age-matched, wild-type littermate mice. Mouse *Tbk1* mRNA was detected at similar levels ($P = 0.83$) in the retinae from the Tg-*TBK1* mice and their wild-type littermates (Fig. 2A). The expression of the human *TBK1* transgene in the retinae of the same mice was similarly assessed using quantitative real-time PCR with probes specific for human *TBK1* mRNA. Robust expression of the human *TBK1* transgene was detected in the retinae of the Tg-*TBK1* mice and was absent from wild-type mice from the same litter (Fig. 2B), demonstrating that the transgene expresses human *TBK1* mRNA and doesn't influence expression of the endogenous ortholog in mouse retinae.

Tg-*TBK1* mice, like human patients with *TBK1*-associated glaucoma, have more than the usual two copies of the *TBK1* gene per genome. We investigated the possibility that increased copies of the *TBK1* gene result in increased production of TBK1 protein in Tg-*TBK1* mice using immunohistochemistry in wild type and Tg-*TBK1* retina. TBK1 protein in wild-type mice is localized within the retinal ganglion cells (Fig. 3A and D), with weaker labelling in the inner and outer nuclear layers. More TBK1 labelling is detected within the retinal ganglion cells of transgenic *TBK1* mice (Fig. 3B and E) than in wild-type littermates (Fig. 3A and D), with similar levels in the other retinal layers. No labelling was detected in a control experiment conducted without primary antibody (Fig. 3C). This pattern of increased TBK1 protein in the retinal ganglion cells of transgenic TBK1 mice was confirmed using two different antibodies and multiple mouse eyes ($n = 8$).

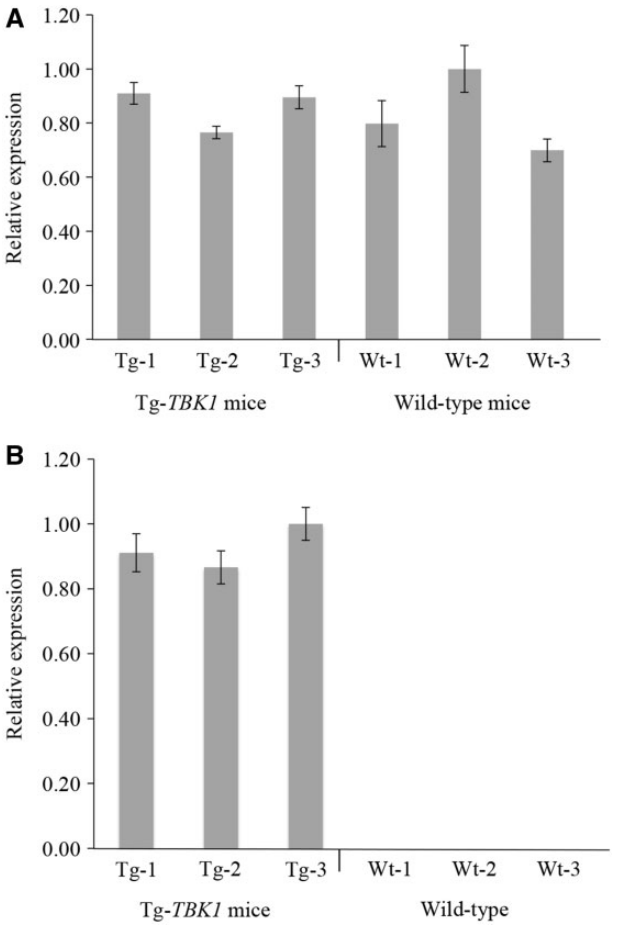

Figure 2. Expression of *TBK1* mRNA in the retinae of Tg-*TBK1* mice. Quantitative real-time PCR was used to measure expression of native mouse *Tbk1* gene (**A**) and the expression of the human *TBK1* transgene (**B**) in both Tg-*TBK1* mice and age-matched wild-type littermates. Expression was normalized to GAPDH. Gene expression is depicted as a fraction of the highest level detected in a sample and the error bars represent standard error.

Transgenic *TBK1* mice have normal IOP

Humans with *TBK1* copy number variations have NTG, glaucoma that occurs without elevated IOP (27–31). Consequently, we measured IOP in transgenic *TBK1* and matched littermates at 5 weeks, 3 months, 7 months, 12 months and 18 months of age (Fig. 4). Transgenic *TBK1* mice have a mean IOP that is within the normal range for C57BL/6J mice (43,44) and indistinguishable from the IOP of matched wild-type littermates ($P > 0.05$) at all ages. These data indicate that transgenic *TBK1* mice have IOPs within the normal range as is expected for an animal model of human NTG.

Tg-*TBK1* mice have progressive retinal ganglion cell loss

A central feature of glaucoma is damage to the retinal ganglion cells and their axons that make up the optic nerve. Animal models are typically assessed for such signs of glaucoma by using quantitative histological methods (i.e., counting retinal ganglion cells) (44–46). We evaluated Tg-*TBK1* mice for a loss of retinal ganglion cells typical of glaucoma using a manual counting strategy. Flat mounts of retinae were prepared from 92 Tg-*TBK1* mice and 96 matched wild-type littermates at a range of ages and retinal ganglion cells were labelled with antibody directed against γ-synuclein.

At 5 weeks of age, there was no difference ($P = 0.82$) between the number of retinal ganglion cells between Tg-*TBK1* mice ($n = 10$) and wild-type littermates ($n = 10$). However, progressive retinal ganglion cell loss was detected as Tg-*TBK1* mice aged (Fig. 5 and Supplementary Material, Fig. S1). A 9% decrease in retinal ganglion cells ($P = 0.00040$) in Tg-*TBK1* mice ($n = 11$) was detected at 3 months of age when compared to wild-type littermates ($n = 10$). Increasing losses of retinal ganglion cells were detected between transgenic mice and control mice aged to 7 months ($n = 50$) and in mice aged to 12 months ($n = 49$). At 18 months of age, Tg-*TBK1* mice ($n = 23$) had a 13% loss of retinal ganglion cells when compared to littermate controls ($n = 25$, $P = 1.5 \times 10^{-8}$).

An intercross of Tg-*TBK1* mice that are hemizygous for the human *TBK1* transgene produced F1 offspring with three genotypes: wild-type (no transgenes), hemizygous (one *TBK1* transgene), or homozygous (two *TBK1* transgenes). Twenty-three F1 mice were aged to 6 months and assessed for glaucoma by manually counting retinal ganglion cells (Fig. 6 and Supplementary Material, Fig. S2). Homozygous mice with two *TBK1* transgenes had 7.6% fewer retinal ganglion cells than hemizygous mice with one *TBK1* transgene and 20% fewer retinal ganglion cells than wild-type littermates ($P = 1.9 \times 10^{-5}$). These experiments demonstrated a dose-response of retinal ganglion cell counts to the number of *TBK1* transgenes. More *TBK1* transgenes resulted in more retinal ganglion cell loss.

We also investigated the retinal ganglion cell counts in the same Tg-*TBK1* mice and matched controls with a second methodology using hematoxylin and eosin (H&E) staining of retinal whole mounts and our previously reported automated image

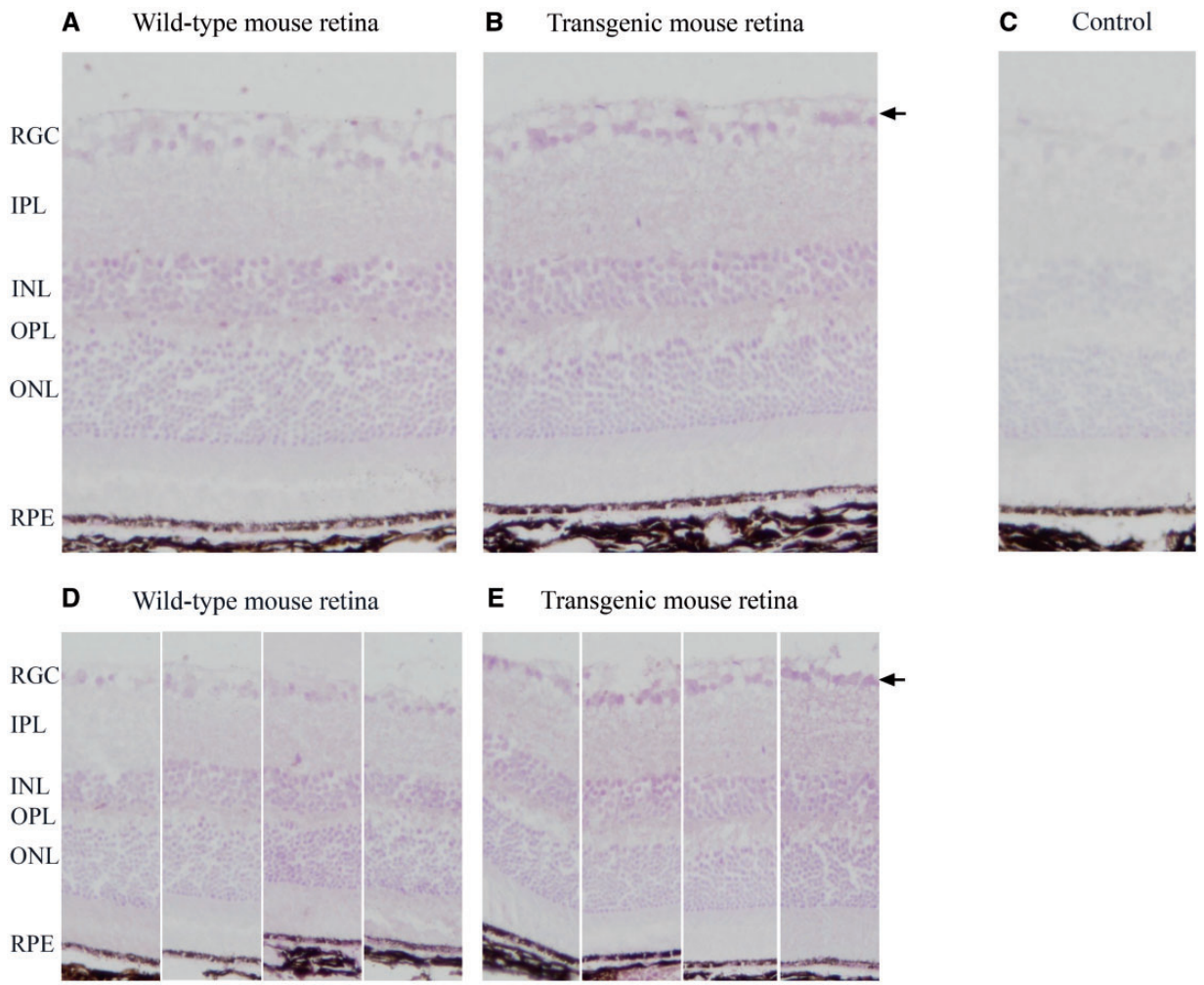

Figure 3. Increased TBK1 protein in the Tg-*TBK1* mouse retina. TBK1 protein is localized in the outer nuclear layer, inner nuclear layer and ganglion cell layer of the retina of Tg-*TBK1* mice and wild-type littermates using immunohistochemistry. (**A**) qualitative increase in labelling of TBK1 protein is apparent in the retinal ganglion cells (indicated with an arrow) of the Tg-*TBK1* mice (**B**) when compared with wild-type litter-mates. A no primary antibody control experiment shows minimal labelling of mouse retina (**C**). Sections of the retina of four Tg-*TBK1* mice (**D**) and four wild-type litter-mates (**E**) also show increased TBK1 protein in the retinal ganglion cells of the transgenic mice (indicated with an arrow). The layers of the mouse retina are indicated with abbreviations: retinal ganglion cell layer (RGC), inner plexiform layer (IPL), inner nuclear layer (INL), outer plexiform layer (OPL), outer nuclear layer (ONL), and retinal pigment epithelium (RPE).

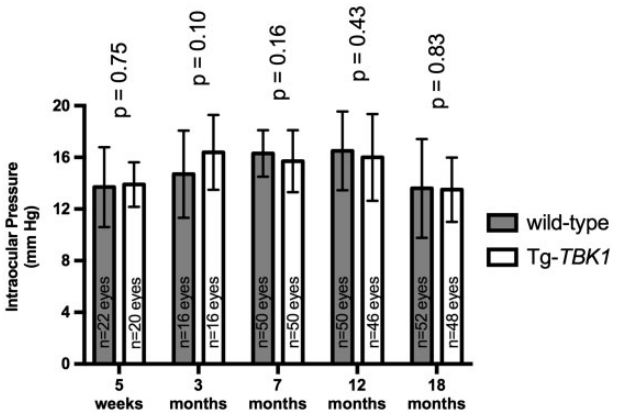

Figure 4. Tg-*TBK1* mice do not have elevated IOP. Transgenic *TBK1* mice have the same IOP as matched wild-type littermate mice at a range of ages ($P > 0.05$). Error bars indicate standard deviation.

analysis algorithm, RetFM-J and RetFM-class (47,48). This approach identifies and counts the ganglion cells, amacrine cells and endothelial cells within the retinal ganglion cell layer based on recognition of features of cell nuclei that differentiate between these cell types. Flat mounts of retinae initially examined with γ-synuclein immuno-labelling were washed, relabelled with H&E and analysed to count retinal ganglion cells with RetFM-Class (Fig. 7 and Supplementary Material, Fig. S3). Retinae from 5-week-old wild-type mice ($n = 3$) and Tg-*TBK1* mice ($n = 2$) had similar retinal ganglion cell counts. When retinae from mice aged to 18 months were analysed, a 11% reduction in ganglion cells ($P = 0.043$) was detected in Tg-*TBK1* mice ($n = 9$) when compared to wild-type littermate mice ($n = 6$). The 11% loss of retinal ganglion cells detected in 18 month old Tg-*TBK1* mice is similar to the 13% measured loss in the same 18 month old Tg-*TBK1* mice using γ-synuclein labelling. Moreover, this analysis indicates that cell loss is largely confined to the retinal ganglion cells in Tg-*TBK1* mice (Supplementary Material, Fig. S3).

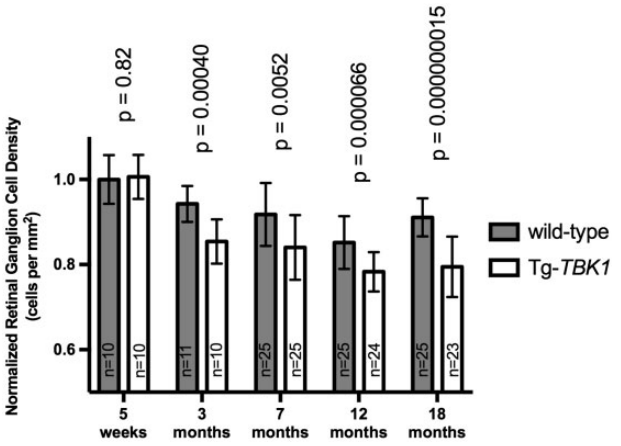

Figure 5. Tg-*TBK1* mice have progressive loss of retinal ganglion cells. Flat mounts of retinae from Tg-*TBK1* and normal littermates were labelled with γ-synuclein and retinal ganglion cell density was determined by manually counting labelled cells. Tg-*TBK1* mice have the same number of retinal ganglion cells as their wild-type littermates when measured shortly after weaning (5 weeks of age). However, the Tg-*TBK1* mice subsequently develop a progressive loss of retinal ganglion cells with 9% fewer cells at 3 months than littermates that increases to 13% fewer cells by 18 months. Data from each time-point was collected as a terminal measurement from different cohorts of mice (total $n = 188$). Error bars indicate standard deviation.

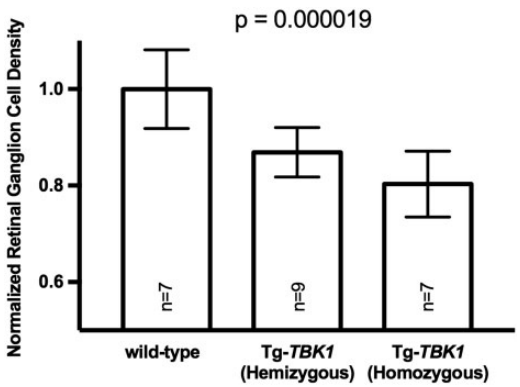

Figure 6. Dose response between the number of *TBK1* transgenes and the loss of retinal ganglion cells. An intercross of Tg-*TBK1* mice (hemizygous for the *TBK1* transgene) produced mice homozygous for the *TBK1* transgene (2 copies); mice hemizygous for the *TBK1* transgene (1 copy); and wild-type mice with no copies of the *TBK1* transgene. Mice were aged to 6 months, flat mounts of their retinae were labelled with γ-synuclein, and retinal ganglion cells were counted. Measurements were normalized to the retinal ganglion cell density determined for the wild-type mice. The number of retinal ganglion cells counted was inversely proportional to the number of *TBK1* transgenes per genome. Hemizygous mice had fewer cells than wild-type littermates and homozygous mice had the fewest cells. Error bars indicate standard deviation.

Discussion

The pathophysiology of retinal ganglion cell death in NTG is complex. Several potential disease processes have been explored including vascular mechanisms (49,50), autoimmune disease (51) and mechanisms involving abnormal intracranial pressure (52,53). The basic causes of NTG have been successfully investigated using a genetic approach. In 2002, Mansoor Sarfarazi discovered the first NTG gene, optineurin (*OPTN*), with linkage studies of a large glaucoma pedigree (22). Missense mutations in *OPTN* were subsequently shown to be responsible for

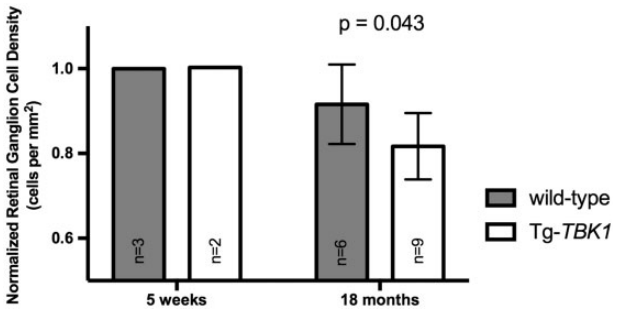

Figure 7. Automated retinal ganglion cell counts of Tg-*TBK1* mice and wild-type littermates using RetFM-J. A subset of retinal whole mounts from mice analysed with γ-synuclein labelling were relabelled with H&E and the density of retinal ganglion cells in these whole mounts was calculated using RetFM-J as previously reported (43). Five-week old Tg-*TBK1* and wild-type mice had similar numbers of retinal ganglion cells, while 18-month old mice Tg-*TBK1* mice had significantly fewer retinal ganglion cells than wildtype littermates. The loss of retinal ganglion cells in 18 month old Tg-*TBK1* mice detected by RetFM-J analysis (11%) is similar to the loss detected by γ-synuclein analysis (13%) depicted in Fig. 5. Error bars indicate standard deviation.

1–2% of NTG cases (23,24). More recently, we discovered that copy number variations of the *TBK1* gene (duplications or triplications) are associated with ∼1% of cases of NTG (27–31). Both *OPTN* and *TBK1* encode proteins that have functions in autophagy and other biological processes including NF-kB signalling. These pedigree-based discoveries have identified a role for autophagy in the pathogenesis of NTG. Both known NTG-causing genes (*TBK1* and *OPTN*) have important functions in autophagy. *TBK1* encodes a kinase that phosphorylates and activates OPTN, while OPTN has been identified as an autophagy receptor that when activated promotes formation of the autophagosome and capture of proteins or structures targeted for degradation (54). These observations and studies suggest that dysregulation of autophagy in key tissues of the eye (i.e., retinal ganglion cells) are important in the development of NTG.

Numerous methods for counting retinal ganglion cells in mice have been employed using protein markers (γ−synuclein, Brn3A), mRNA markers (*Sncg*), histological staining patterns (Nissl and H&E) and retrograde labelling from axonal termini (47,48,55–59). Each has strengths and weaknesses with regards to sensitivity, specificity and technical limitations of the method (56,57,60). We used two methods to identify and count retinal ganglion cells. First, the cells labelled with γ−synuclein antibody were manually counted. Second, retinal ganglion cells stained with H&E were automatically counted based on nuclear features using the RetFM-Class algorithm. The reduction in retinal ganglion cell density measured in Tg-*TBK1* mice by both methods is strikingly similar.

We previously demonstrated that TBK1 is specifically localized to the retinal ganglion cells in the human retina (27,61). In this report, we identify native mouse *Tbk1* in the inner and outer nuclear layer cells as well as in the retinal ganglion cells in the retinae of wild-type and Tg-*TBK1* mice. However, increased labelling of this kinase protein is recognized in the retinal ganglion cells of Tg-*TBK1* mice. These data suggest that human TBK1 protein produced by the *TBK1* transgene may be somewhat confined to the retinal ganglion cells in Tg-*TBK1* mice, mimicking the localization of native TBK1 protein in human retina. This expression pattern suggests that the Tg-*TBK1* mouse is a good model of human NTG caused by CNVs of the

TBK1 gene. Moreover, analysis of aging Tg-*TBK1* mice shows a significant loss of retinal ganglion cells over time.

Other transgenic models of NTG have also been created to model human disease. A missense mutation (E50K) in *OPTN* has been strongly associated with human glaucoma. In one transgenic mouse model, overexpression of the E50K OPTN mutant protein in mice resulted in features of NTG including thinning of all retinal layers and diffuse retinal apoptosis that occurred without elevated IOP. Diffuse apoptosis was detected in all cell types of the retina, which suggests that overexpression of OPTN mutants has a range of effects on retina (62). Another transgenic mouse made with an E50K optineurin transgene also showed signs of NTG. These mice had loss of retinal ganglion cells, loss of optic nerve axons and reduced visually evoked potentials (63). Transgenic *OPTN* mice along with transgenic Tg-*TBK1* mice are powerful tools for investigating the pathogenesis of glaucoma. Recent studies of transgenic *OPTN* mice have suggested that autophagy involving mitochondria (mitophagy) may have an important role in glaucoma (64).

In sum, the evidence linking *TBK1* with NTG is growing. *TBK1* copy number variations have been detected in NTG patients in multiple studies. Five additional studies of NTG patients (28–31) have replicated the discovery that *TBK1* CNVs are associated with approximately 1 in 100 cases of NTG (27). Some preliminary studies have shown that duplication of the *TBK1* gene has functional consequences including increased transcription of *TBK1* mRNA (27) and activation of autophagy (37) in cell culture systems. However, in the current report, we provide the most compelling evidence that *TBK1* copy number variations are pathogenic. We engineered Tg-*TBK1* mice to have the same genetic defect (an extra dose of the *TBK1* gene) as our human NTG patients with *TBK1* gene duplications. Subsequently, we showed that Tg-*TBK1* mice have a progressive loss of retinal ganglion cells that occurs without elevated IOP. Tg-*TBK1* mice recapitulate human glaucoma and provide the strongest proof that CNVs involving the *TBK1* gene cause glaucoma. Further study of these and other mice may provide new insights into the mechanisms by which autophagy genes lead to retinal ganglion cell damage and glaucoma. Moreover, this line of investigation has great potential for informing the development of novel therapies that are targeted to the specific causes of glaucoma.

Materials and Methods

Mouse husbandry

All animals were treated in accordance with the ARVO Statement for the Use of Animals in Ophthalmic and Vision Research. All experimental protocols were approved by the Animal Care and Use Committee of the University of Iowa. C57BL/6J mice were obtained from The Jackson Laboratory (Bar Harbor, ME). All mice were housed and bred at the University of Iowa Research Animal Facility. Mice were maintained on a 4% fat NIH 31 diet provided ad libitum and were housed in cages containing dry bedding (Cellu-dri; Shepherd Specialty Papers, Kalamazoo, MI). The environment was kept at 21 °C with a 12-h light/12-h dark cycle.

Generation of Tg-TBK1 transgenic mice

A bacterial artificial chromosome (RP11-60O8) containing the wild-type human *TBK1* gene (natural promoter, exons and introns) was purchased from BACPAC (Oakland, CA) and was injected into C57BL/6J/SJL hybrid embryos in collaboration with the Transgenic Animal Facility at the University of Iowa. One resultant founder mouse was found to have a single human *TBK1* transgene integrated into its genome. The founder and its offspring were backcrossed to C57BL/6J mice for seven generations by the onset of this study (>10 generations by the conclusion of the study). The integration of a single BAC (1 copy of the human *TBK1* gene) was confirmed using a commercially available real-time PCR assay (TaqMan, *TBK1* test probe Hs06980763, *Tfrc* reference probe 4458370, Thermo Fisher) and a CFX96 real time PCR machine (BioRad Laboratories, Hercules, CA) following the manufacturer's protocol. All mice were tested using this assay and those mice with the *TBK1* transgene were termed 'Tg-*TBK1* mice'.

Gene expression studies

Retinae were harvested from Tg-*TBK1* and age-matched wild-type mice of the same litter. Both retinas from each mouse were pooled together in a tube and flash frozen in liquid nitrogen for each animal. Total RNA was extracted using the RNeasy Mini Kit (Qiagen, Valencia, CA) and cDNA was synthesized using the BioRad iScript cDNA Synthesis Kit (Bio-Rad Laboratories, Hercules, CA). Quantitative polymerase chain reaction was done using TaqMan Gene Expression probes (*TBK1* test probe Hs00975477_m1, mouse *Tbk1* test probe Mm00451150_m1, and *Gapdh* reference probe Mm99999915_g1, Thermo Fisher) following the manufacturer's protocol. Each retinal cDNA library was amplified in triplicate in two separate experiments. Relative gene expression was calculated by the BioRad CFX Manager software. Gene expression levels were normalized using mGAPDH as the reference probe and reported as relative expression with the sample with the highest expression level set at 100%. The relative expression levels of mouse *Tbk1* (quantitation cycle, C_q) were compared between Tg-*TBK1* and wild-type littermate mice using a two-tailed paired *t*-test.

Immunohistochemistry

Mice were euthanized using CO_2 asphyxiation followed by cervical dislocation. The eyes were placed in 4% paraformaldehyde for >4 h at 4°C and then stored in PBS. The anterior segment and the lens were removed and eye cups were then infiltrated in sucrose solution and embedded in OCT compound. The eyes were then cut into 7 μm sections on a cryostat (MICROM GmbH, Walldorf, Germany). Sections were incubated in blocking solution (1:50 dilution of blocking serum from Vectastain ABC Kit, Vector Laboratories, Burlingame, CA) for 30 min then in 1:500 anti-Tbk1 antibody (AbCam, Cambridge, MA) for 1 h. Sections were washed 3X with PBS and then incubated with biotinylated secondary antibody for 30 min (1:100 dilution from Vector Laboratories, Burlingame, CA). Following washes with PBS (3 × 5 min), sections were incubated in Vectastain ABC reagents (1:50 dilution reagent A and 1:50 dilution reagent B from Vectastain ABC Kit) for 30 min and then washed with PBS (3 × 5 min). Sections were then treated with avidin biotin horseradish peroxidase substrate (Vector VIP substrate kit, Vector Laboratories). Images were obtained using an Olympus BX41 microscope with a 20X objective. Sections of retinae from transgenic and wild-type littermate mice were developed in parallel under identical conditions, identical microscope settings and identical camera settings.

Measurement of IOP

IOP was measured using a rebound tonometer as previously described (65). Mice were acclimated to the procedure room, anaesthetized with 2.5% isoflurane + 100% oxygen, and IOP was measured with a TonoLab tonometer (Colonial Medical Supply, Franconia, NH). All IOP cohorts included male and female mice.

Retinal ganglion cell counts

Retinal whole mounts of transgenic mice and littermates were prepared and retinal ganglion cells counted as previously described (66). Whole-mount preparations of retinas were incubated with 0.3% Triton X-100 for 4 h and were blocked with 0.1% filtered BSA solution with 0.1% Triton X-100 for 1 h. These retinae were then incubated with 1:300 anti-γ-synuclein antibody (AbCam, Cambridge, MA) overnight, followed by incubation with secondary antibody Alexa Fluor 488 (Life Technologies, Madison, WI) for 30 min. For counting, four images of the mid-peripheral region were captured (one from each quadrant) at 100X magnification using an Olympus BX41 microscope. γ-Synuclein–positive cells were counted in a 10,355 μm^2 area of each image using ImageJ software (NIH). Technicians were masked to the genotypes of the mice. Cell counts were compared between Tg-*TBK1* mice and matched normal littermates for each time point using a two-tailed *t*-test. Differences with $P < 0.05$ were considered significant.

Retinal whole mounts from some of the mice that were studied with immunohistochemical labelling were also reanalysed using a semi-automated image analysis software package, RetFM-Class, that classifies cells of the retinal ganglion cell layer as previously described (47,48). Briefly, whole mounts were washed in PBS and labelled with haematoxylin and eosin. Images of the retinal ganglion cell layer were obtained with a light microscope (BX52; Olympus, Tokyo, Japan) using a digital camera (DP72; Olympus, Tokyo, Japan). CellSens Standard imaging software (Olympus, Tokyo, Japan) was used for capturing colour images (RGB mode, .tif format), using fixed software settings for all images. Exposures were normalized using white balance and 1% spot option of the region tool before capturing images. The CellSens Extended Focal Imaging module was used as needed to correct for unevenness in the z-plane due to variable topography of whole-mounted retinae. Images were captured from each retinal whole mount in fixed topographic locations. Two images were captured from three regions (peripheral, mid-peripheral and central) of each of four retinal leaflets, for a total of 24 images per retina. Raw images from each retina were manually reviewed and regions containing artefacts (such as stain precipitate, tears and debris) were manually excluded from each image, and nuclei counts of each image obtained using RetFM-J. A minimum of two retinal leaflets per whole mounted retina were required for inclusion in the analysis. Many retinae that were successfully analysed with the γ-synuclein were excluded from the RetFM-Class approach because they did not survive the re-mounting and re-staining process. Retinal areas were measured for each retina as previously described (47) and retinal ganglion cell densities were computed for each whole mount as mathematical averages of all images analysed per experiment (Fig. 7). Raw data from retinal ganglion cell layer analyses are plotted for each animal (Supplementary Material, Fig. S3).

Supplementary Material

Supplementary Material is available at *HMG* online.

Conflict of Interest statement. None declared.

Funding

This work was supported by the National Institutes of Health [R01 EY023512]; American Glaucoma Society [Mid-Career Award]; the Glaucoma Research Foundation [Frank Stein and Paul S. May Grant for Innovative Glaucoma Research]; Research to Prevent Blindness [Physician-Scientist Award]; and Casey Mahon.

References

1. Quigley, H.A. and Broman, A.T. (2006) The number of people with glaucoma worldwide in 2010 and 2020. *Br. J. Ophthalmol.*, **90**, 262–267.
2. Kim, K.E. and Park, K.H. (2016) Update on the Prevalence, Etiology, Diagnosis, and Monitoring of Normal-Tension Glaucoma. *Asia Pac. J. Ophthalmol. (Phila)*, **5**, 23–31.
3. Cho, H.K. and Kee, C. (2014) Population-based glaucoma prevalence studies in Asians. *Surv. Ophthalmol.*, **59**, 434–447.
4. Fingert, J.H. (2011) Primary open-angle glaucoma genes. *Eye*, **25**, 587–595.
5. Thorleifsson, G., Walters, G.B., Hewitt, A.W., Masson, G., Helgason, A., Dewan, A., Sigurdsson, A., Jonasdottir, A., Gudjonsson, S.A., Magnusson, K.P., *et al.* (2010) Common variants near CAV1 and CAV2 are associated with primary open-angle glaucoma. *Nat. Genet.*, **42**, 906–909.
6. Burdon, K.P., MacGregor, S., Hewitt, A.W., Sharma, S., Chidlow, G., Mills, R.A., Danoy, P., Casson, R., Viswanathan, A.C., Liu, J.Z., *et al.* (2011) Genome-wide association study identifies susceptibility loci for open angle glaucoma at TMCO1 and CDKN2B-AS1. *Nat. Genet.*, **43**, 574–578.
7. Ramdas, W.D., van Koolwijk, L.M.E., Lemij, H.G., Pasutto, F., Cree, A.J., Thorleifsson, G., Janssen, S.F., Jacoline, T.B., Amin, N., Rivadeneira, F., *et al.* (2011) Common genetic variants associated with open-angle glaucoma. *Hum. Mol. Genet.*, **20**, 2464–2471.
8. Wiggs, J.L., Yaspan, B.L., Hauser, M.A., Kang, J.H., Allingham, R.R., Olson, L.M., Abdrabou, W., Fan, B.J., Wang, D.Y., Brodeur, W., *et al.* (2012) Common variants at 9p21 and 8q22 are associated with increased susceptibility to optic nerve degeneration in glaucoma. *PLoS Genet.*, **8**, e1002654.
9. Mabuchi, F., Sakurada, Y., Kashiwagi, K., Yamagata, Z., Iijima, H. and Tsukahara, S. (2012) Association between Genetic Variants Associated with Vertical Cup-to-Disc Ratio and Phenotypic Features of Primary Open-Angle Glaucoma. *Ophthalmology*, **119**, 1819–1825.
10. Gharahkhani, P., Burdon, K.P., Fogarty, R., Sharma, S., Hewitt, A.W., Martin, S., Law, M.H., Cremin, K., Bailey, J.N.C., Loomis, S.J., *et al.* (2014) Common variants near ABCA1, AFAP1 and GMDS confer risk of primary open-angle glaucoma. *Nat. Genet.*, **46**, 1120–1125.
11. Chen, Y., Lin, Y., Vithana, E.N., Jia, L., Zuo, X., Wong, T.Y., Chen, L.J., Zhu, X., Tam, P.O.S., Gong, B., *et al.* (2014) Common variants near ABCA1 and in PMM2 are associated with primary open-angle glaucoma. *Nat. Genet.*, **46**, 1115–1119.
12. Hysi, P.G., Cheng, C.Y., Springelkamp, H., MacGregor, S., Bailey, J.N.C., Wojciechowski, R., Vitart, V., Nag, A., Hewitt, A.W., Höhn, R., *et al.* (2014) Genome-wide analysis

of multi-ancestry cohorts identifies new loci influencing intraocular pressure and susceptibility to glaucoma. *Nat. Genet.*, **46**, 1126–1130.
13. Bailey, J.N.C., Loomis, S.J., Kang, J.H., Allingham, R.R., Gharahkhani, P., Khor, C.C., Burdon, K.P., Aschard, H., Chasman, D.I., Igo, R.P., *et al.* (2016) Genome-wide association analysis identifies TXNRD2, ATXN2 and FOXC1 as susceptibility loci for primary open-angle glaucoma. *Nat. Genet.*, **48**, 189–194.
14. Writing Committee for the Normal Tension Glaucoma Genetic Study Group of Japan Glaucoma Society, Meguro, A., Inoko, H., Ota, M., Mizuki, N. and Bahram, S. (2010) Genome-wide association study of normal tension glaucoma: common variants in SRBD1 and ELOVL5 contribute to disease susceptibility. *Ophthalmology*, **117**, 1331–1338.
15. Shibuya, E., Meguro, A., Ota, M., Kashiwagi, K., Mabuchi, F., Iijima, H., Kawase, K., Yamamoto, T., Nakamura, M., Negi, A., *et al.* (2008) Association of Toll-like receptor 4 gene polymorphisms with normal tension glaucoma. *Invest. Ophthalmol. Vis. Sci.*, **49**, 4453–4457.
16. Takamoto, M., Kaburaki, T., Mabuchi, A., Araie, M., Amano, S., Aihara, M., Tomidokoro, A., Iwase, A., Mabuchi, F., Kashiwagi, K., *et al.* (2012) Common variants on chromosome 9p21 are associated with normal tension glaucoma. *PLoS One*, **7**, e40107.
17. Burdon, K.P., Crawford, A., Casson, R.J., Hewitt, A.W., Landers, J., Danoy, P., Mackey, D.A., Mitchell, P., Healey, P.R. and Craig, J.E. (2012) Glaucoma Risk Alleles at CDKN2B-AS1 Are Associated with Lower Intraocular Pressure, Normal-Tension Glaucoma, and Advanced Glaucoma. *Ophthalmology*, **119**, 1539–1545.
18. Wiggs, J.L. (2015) Glaucoma Genes and Mechanisms. *Prog. Mol. Biol. Transl Sci.*, **134**, 315–342.
19. Stone, E.M., Fingert, J.H., Alward, W.L.M., Nguyen, T.D., Polansky, J.R., Sunden, S.L.F., Nishimura, D., Clark, A.F., Nystuen, A., Nichols, B.E., *et al.* (1997) Identification of a Gene That Causes Primary Open Angle Glaucoma. *Science*, **275**, 668–670.
20. Alward, W.L., Fingert, J.H., Coote, M.A., Johnson, A.T., Lerner, S.F., Junqua, D., Durcan, F.J., McCartney, P.J., Mackey, D.A., Sheffield, V.C., *et al.* (1998) Clinical features associated with mutations in the chromosome 1 open-angle glaucoma gene (GLC1A). *N. Engl. J. Med.*, **338**, 1022–1027.
21. Fingert, J.H., Héon, E., Liebmann, J.M., Yamamoto, T., Craig, J.E., Rait, J., Kawase, K., Hoh, S.T., Buys, Y.M., Dickinson, J., *et al.* (1999) Analysis of myocilin mutations in 1703 glaucoma patients from five different populations. *Hum. Mol. Genet.*, **8**, 899–905.
22. Rezaie, T., Child, A., Hitchings, R., Brice, G., Miller, L., Coca-Prados, M., Héon, E., Krupin, T., Ritch, R., Kreutzer, D., *et al.* (2002) Adult-onset primary open-angle glaucoma caused by mutations in optineurin. *Science*, **295**, 1077–1079.
23. Aung, T., Ebenezer, N.D., Brice, G., Child, A.H., Prescott, Q., Lehmann, O.J., Hitchings, R.A. and Bhattacharya, S.S. (2003) Prevalence of optineurin sequence variants in adult primary open angle glaucoma: implications for diagnostic testing. *J. Med. Genet.*, **40**, e101.
24. Alward, W.L.M., Kwon, Y.H., Kawase, K., Craig, J.E., Hayreh, S.S., Johnson, A.T., Khanna, C.L., Yamamoto, T., Mackey, D.A., Roos, B.R., *et al.* (2003) Evaluation of optineurin sequence variations in 1,048 patients with open-angle glaucoma. *Am. J. Ophthalmol.*, **136**, 904–910.
25. Aung, T., Rezaie, T., Okada, K., Viswanathan, A.C., Child, A.H., Brice, G., Bhattacharya, S.S., Lehmann, O.J., Sarfarazi, M. and Hitchings, R.A. (2005) Clinical features and course of patients with glaucoma with the E50K mutation in the optineurin gene. *Invest. Ophthalmol. Vis. Sci.*, **46**, 2816–2822.
26. Hauser, M.A., Sena, D.F., Flor, J., Walter, J., Auguste, J., LaRocque-Abramson, K., Graham, F., DelBono, E., Haines, J.L., Pericak-Vance, M.A., *et al.* (2006) Distribution of optineurin sequence variations in an ethnically diverse population of low-tension glaucoma patients from the United States. *J. Glaucoma*, **15**, 358–363.
27. Fingert, J.H., Robin, A.L., Roos, B.R., Davis, L.K., Scheetz, T.E., Wassink, T.H., Kwon, Y.H., Alward, W.L.M., Mullins, R.F., Sheffield, V.C., *et al.* (2011) Copy number variations on chromosome 12q14 in patients with normal tension glaucoma. *Hum. Mol. Genet.*, **20**, 2482–2494.
28. Kawase, K., Allingham, R.R., Meguro, A., Mizuki, N., Roos, B., Solivan-Timpe, F.M., Robin, A.L., Ritch, R. and Fingert, J.H. (2012) Confirmation of TBK1 duplication in normal tension glaucoma. *Exp. Eye Res.*, **96**, 178–180.
29. Ritch, R., Darbro, B., menon, G., Khanna, C.L., Solivan-Timpe, F., Roos, B.R., Sarfarzi, M., Kawase, K., Yamamoto, T., Robin, A.L., *et al.* (2014) TBK1 Gene Duplication and Normal-Tension Glaucoma. *JAMA Ophthalmol.*, **132**, 544–548.
30. Awadalla, M.S., Fingert, J.H., Roos, B.E., Chen, S., Holmes, R., Galanopolous, A., Ridge, B., Souzeau, E., Siggs, O.M., Hewitt, A.W., *et al.* (2015) Copy Number Variations of TBK1 in Australian Patients With Primary Open-Angle Glaucoma. *Am J Ophthalmol.*, **159**, 124–130. e1.
31. Liu, Y., Garrett, M.E., Yaspan, B.L., Bailey, J.C., Loomis, S.J., Brilliant, M., Budenz, D.L., Christen, W.G., Fingert, J.H., Gaasterland, D., *et al.* (2014) DNA copy number variants of known glaucoma genes in relation to primary open-angle glaucoma. *Invest Ophthalmol. Vis. Sci.*, **55**, 8251–8258.
32. McDonald, K.K., Abramson, K., Beltran, M.A., Ramirez, M.G., Alvarez, M., Ventura, A., Santiago-Turla, C., Schmidt, S., Hauser, M.A. and Allingham, R.R. (2010) Myocilin and optineurin coding variants in Hispanics of Mexican descent with POAG. *J. Hum. Genet.*, **55**, 697–700.
33. Galluzzi, L., Kepp, O. and Kroemer, G. (2011) Autophagy and innate immunity ally against bacterial invasion. *Embo J.*, **30**, 3213–3214.
34. Park, H.Y.L., Kim, J.H. and Park, C.K. (2012) Activation of autophagy induces retinal ganglion cell death in a chronic hypertensive glaucoma model. *Cell Death Dis.*, **3**, e290.
35. Piras, A., Gianetto, D., Conte, D., Bosone, A. and Vercelli, A. (2011) Activation of autophagy in a rat model of retinal ischemia following high intraocular pressure. *PLoS One*, **6**, e22514.
36. Dietz, J.A., Maes, M.E., Huang, S., Yandell, B.S., Schlamp, C.L., Montgomery, A.D., Allingham, R.R., Hauser, M.A. and Nickells, R.W. (2014) Spink2 modulates apoptotic susceptibility and is a candidate gene in the Rgcs1 QTL that affects retinal ganglion cell death after optic nerve damage. *PLoS One*, **9**, e93564.
37. Tucker, B.A., Solivan-Timpe, F., Roos, B.R., Anfinson, K.R., Robin, A.L., Wiley, L.A., Mullins, R.F. and Fingert, J.H. (2014) Duplication of TBK1 stimulates autophagy in iPSC-derived retinal cells from a patient with normal tension glaucoma. *J. Stem Cell Res. Ther.*, **3**, 161.
38. Ghavami, S., Shojaei, S., Yeganeh, B., Ande, S.R., Jangamreddy, J.R., Mehrpour, M., Christoffersson, J., Chaabane, W., Moghadam, A.R., Kashani, H.H., *et al.* (2014) Autophagy and apoptosis dysfunction in neurodegenerative disorders. *Prog. Neurobiol.*, **112**, 24–49.

39. Freischmidt, A., Wieland, T., Richter, B., Ruf, W., Schaeffer, V., Müller, K., Marroquin, N., Nordin, F., Hübers, A., Weydt, P., *et al.* (2015) Haploinsufficiency of TBK1 causes familial ALS and fronto-temporal dementia. *Nat. Neurosci.*, **18**, 631–636.
40. Cirulli, E.T., Lasseigne, B.N., Petrovski, S., Sapp, P.C., Dion, P.A., Leblond, C.S., Couthouis, J., Lu, Y.F., Wang, Q., Krueger, B.J., *et al.* (2015) Exome sequencing in amyotrophic lateral sclerosis identifies risk genes and pathways. *Science*, **347**, 1436–1441.
41. Maruyama, H., Morino, H., Ito, H., Izumi, Y., Kato, H., Watanabe, Y., Kinoshita, Y., Kamada, M., Nodera, H., Suzuki, H., *et al.* (2010) Mutations of optineurin in amyotrophic lateral sclerosis. *Nature*, **465**, 223–226.
42. Elden, A.C., Kim, H.J., Hart, M.P., Chen-Plotkin, A.S., Johnson, B.S., Fang, X., Armakola, M., Geser, F., Greene, R., Lu, M.M., *et al.* (2010) Ataxin-2 intermediate-length polyglutamine expansions are associated with increased risk for ALS. *Nature*, **466**, 1069–1075.
43. Savinova, O.V., Sugiyama, F., Martin, J.E., Tomarev, S.I., Paigen, B.J., Smith, R.S. and John, S.W. (2001) Intraocular pressure in genetically distinct mice: an update and strain survey. *BMC Genet.*, **2**, 12.
44. Trantow, C.M., Mao, M., Petersen, G.E., Alward, E.M., Alward, W.L.M., Fingert, J.H. and Anderson, M.G. (2009) Lyst mutation in mice recapitulates iris defects of human exfoliation syndrome. *Invest. Ophthalmol. Vis. Sci.*, **50**, 1205–1214.
45. John, S.W., Smith, R.S., Savinova, O.V., Hawes, N.L., Chang, B., Turnbull, D., Davisson, M., Roderick, T.H. and Heckenlively, J.R. (1998) Essential iris atrophy, pigment dispersion, and glaucoma in DBA/2J mice. *Invest. Ophthalmol. Vis. Sci.*, **39**, 951–962.
46. Mao, M., Hedberg-Buenz, A., Koehn, D., John, S.W.M. and Anderson, M.G. (2011) Anterior segment dysgenesis and early-onset glaucoma in nee mice with mutation of Sh3pxd2b. *Invest. Ophthalmol. Vis. Sci.*, **52**, 2679–2688.
47. Hedberg-Buenz, A., Christopher, M.A., Lewis, C.J., Meyer, K.J., Rudd, D.S., Dutca, L.M., Wang, K., Garvin, M.K., Scheetz, T.E., Abràmoff, M.D., *et al.* (2015) RetFM-J, an ImageJ-based module for automated counting and quantifying features of nuclei in retinal whole-mounts. *Exp. Eye Res.*, 10.1016/j.exer.2015.07.020.
48. Hedberg-Buenz, A., Christopher, M.A., Lewis, C.J., Fernandes, K.A., Dutca, L.M., Wang, K., Scheetz, T.E., Abràmoff, M.D., Libby, R.T., Garvin, M.K., *et al.* (2015) Quantitative measurement of retinal ganglion cell populations via histology-based random forest classification. *Exp. Eye Res.*, 10.1016/j.exer.2015.09.011.
49. Hayreh, S.S., Revie, I.H. and Edwards, J. (1970) Vasogenic origin of visual field defects and optic nerve changes in glaucoma. *Br. J. Ophthalmol.*, **54**, 461–472.
50. Hayreh, S.S. (2001) Blood flow in the optic nerve head and factors that may influence it. *Prog. Retin. Eye Res.*, **20**, 595–624.
51. Bell, K., Gramlich, O.W.,Thun Und Hohenstein-Blaul,Von, N., Beck, S., Funke, S., Wilding, C., Pfeiffer, N. and Grus, F.H. (2013) Does autoimmunity play a part in the pathogenesis of glaucoma?. *Prog. Retin. Eye Res.*, **36**, 199–216.
52. Berdahl, J.P., Allingham, R.R. and Johnson, D.H. (2008) Cerebrospinal fluid pressure is decreased in primary open-angle glaucoma. *Ophthalmology*, **115**, 763–768.
53. Berdahl, J.P., Fautsch, M.P., Stinnett, S.S. and Allingham, R.R. (2008) Intracranial pressure in primary open angle glaucoma, normal tension glaucoma, and ocular hypertension: a case-control study. *Invest. Ophthalmol. Vis. Sci.*, **49**, 5412–5418.
54. Wild, P., Farhan, H., McEwan, D.G., Wagner, S., Rogov, V.V., Brady, N.R., Richter, B., Korac, J., Waidmann, O., Choudhary, C., *et al.* (2011) Phosphorylation of the autophagy receptor optineurin restricts Salmonella growth. *Science*, **333**, 228–233.
55. Quigley, H.A., Cone, F.E., Gelman, S.E., Yang, Z., Son, J.L., Oglesby, E.N., Pease, M.E. and Zack, D.J. (2011) Lack of neuroprotection against experimental glaucoma in c-Jun N-terminal kinase 3 knockout mice. *Exp. Eye Res.*, **92**, 299–305.
56. Schlamp, C.L., Montgomery, A.D., Mac Nair, C.E., Schuart, C., Willmer, D.J. and Nickells, R.W. (2013) Evaluation of the percentage of ganglion cells in the ganglion cell layer of the rodent retina. *Mol. Vis.*, **19**, 1387–1396.
57. Soto, I., Oglesby, E., Buckingham, B.P., Son, J.L., Roberson, E.D.O., Steele, M.R., Inman, D.M., Vetter, M.L., Horner, P.J. and Marsh-Armstrong, N. (2008) Retinal ganglion cells downregulate gene expression and lose their axons within the optic nerve head in a mouse glaucoma model. *J. Neurosci.*, **28**, 548–561.
58. Liu, Y., McDowell, C.M., Zhang, Z., Tebow, H.E., Wordinger, R.J. and Clark, A.F. (2014) Monitoring retinal morphologic and functional changes in mice following optic nerve crush. *Invest. Ophthalmol. Vis. Sci.*, **55**, 3766–3774.
59. Danias, J., Lee, K.C., Zamora, M.F., Chen, B., Shen, F., Filippopoulos, T., Su, Y., Goldblum, D., Podos, S.M. and Mittag, T. (2003) Quantitative analysis of retinal ganglion cell (RGC) loss in aging DBA/2NNia glaucomatous mice: comparison with RGC loss in aging C57/BL6 mice. *Invest. Ophthalmol. Vis. Sci.*, **44**, 5151–5162.
60. Mead, B., Thompson, A., Scheven, B.A., Logan, A., Berry, M. and Leadbeater, W. (2014) Comparative evaluation of methods for estimating retinal ganglion cell loss in retinal sections and wholemounts. *PLoS One*, **9**, e110612.
61. Fingert, J.H., darbro, B.W., Qian, Q., Van Rheeden, R., Miller, K., Riker, M., Solivan-Timpe, F., Roos, B.R., Robin, A.L. and Mullins, R.F. (2013) *TBK1* and flanking genes in human retina. *Ophthalmic Genet.*, 10.3109/13816810.2013.768674.
62. Minegishi, Y., Iejima, D., Kobayashi, H., Chi, Z.L., Kawase, K., Yamamoto, T., Seki, T., Yuasa, S., Fukuda, K. and Iwata, T. (2013) Enhanced optineurin E50K-TBK1 interaction evokes protein insolubility and initiates familial primary open-angle glaucoma. *Hum. Mol. Genet.*, **22**, 3559–3567.
63. Tseng, H.C., Riday, T.T., McKee, C., Braine, C.E., Bomze, H., Barak, I., Marean-Reardon, C., John, S.W.M., Philpot, B.D. and Ehlers, M.D. (2015) Visual impairment in an optineurin mouse model of primary open-angle glaucoma. *Neurobiol. Aging*, **36**, 2201–2212.
64. Shim, M.S., Takihara, Y., Kim, K.Y., Iwata, T., Yue, B.Y.J.T., Inatani, M., Weinreb, R.N., Perkins, G.A. and Ju, W.K. (2016) Mitochondrial pathogenic mechanism and degradation in optineurin E50K mutation-mediated retinal ganglion cell degeneration. *Sci. Rep.*, **6**, 33830.
65. Kim, C.Y., Kuehn, M.H., Anderson, M.G. and Kwon, Y.H. (2007) Intraocular pressure measurement in mice: a comparison between Goldmann and rebound tonometry. *Eye (Lond)*, **21**, 1202–1209.
66. Zode, G.S., Kuehn, M.H., Nishimura, D.Y., Searby, C.C., Mohan, K., Grozdanic, S.D., Bugge, K., Anderson, M.G., Clark, A.F., Stone, E.M., *et al.* (2011) Reduction of ER stress via a chemical chaperone prevents disease phenotypes in a mouse model of primary open angle glaucoma. *J. Clin. Invest.*, **121**, 3542–3553.